

Field angle dependent change of the magnetization reversal mode in epitaxial Co (0001) films

A. K. Suszka, A. Etxebarria, O. Idigoras, D. Cortés-Ortuño, P. Landeros, and A. Berger

Citation: [Applied Physics Letters](#) **105**, 222402 (2014); doi: 10.1063/1.4903060

View online: <http://dx.doi.org/10.1063/1.4903060>

View Table of Contents: <http://scitation.aip.org/content/aip/journal/apl/105/22?ver=pdfcov>

Published by the [AIP Publishing](#)

Articles you may be interested in

[Direct observation of magnetization reversal and low field magnetoresistance of epitaxial La_{0.7}Sr_{0.3}MnO₃/SrTiO₃ \(001\) thin films at room temperature](#)

[J. Appl. Phys.](#) **112**, 013906 (2012); 10.1063/1.4730966

[Magnetic coercivity of focused ion beam irradiated lines in a Pt/Co\(1.4 nm\)/Pt film](#)

[J. Appl. Phys.](#) **109**, 093919 (2011); 10.1063/1.3580506

[Time dependence of magnetization reversal influenced by current in perpendicularly magnetized Co/Pt thin film](#)

[J. Appl. Phys.](#) **104**, 083907 (2008); 10.1063/1.3002419

[Magnetization reversal in Co/Pd nanostructures and films](#)

[J. Appl. Phys.](#) **97**, 10J702 (2005); 10.1063/1.1849572

[Reorientational magnetic transition in nanostructured epitaxial cobalt patches \(abstract\)](#)

[J. Appl. Phys.](#) **81**, 5470 (1997); 10.1063/1.364628

An advertisement for KeySight B2980A Series Picoammeters/Electrometers. The ad features a red border with a white background. On the left, text reads 'Confidently measure down to 0.01 fA and up to 10 PΩ' and 'Keysight B2980A Series Picoammeters/Electrometers'. Below this is a red button with the text 'View video demo'. On the right, there is an image of the device and the KeySight Technologies logo.

Field angle dependent change of the magnetization reversal mode in epitaxial Co (0001) films

A. K. Suszka,^{1,a)} A. Etxebarria,¹ O. Idigoras,¹ D. Cortés-Ortuño,^{2,b)} P. Landeros,² and A. Berger¹

¹CIC nanoGUNE Consolider, E-20018 Donostia-San Sebastian, Spain

²Departamento de Física, Universidad Técnica Federico Santa María, Avenida España 1680, 2390123 Valparaíso, Chile

(Received 17 October 2014; accepted 15 November 2014; published online 1 December 2014)

The magnetic field dependent reorientation phase transition of epitaxial Co (0001) films with perpendicular magnetic anisotropy is studied as a function of the applied field angle. The experimental data reveal an abrupt qualitative change of the magnetization reversal path at a critical angle between in-plane and out-of-plane field orientation, which is caused by a change in the domain formation process occurring concurrently with the phase transition. By means of our experiments and model calculations, we demonstrate that the observations are due to a transition from instability driven magnetization reversal occurring near in-plane field orientation to domain nucleation processes, which occur near out-of-plane orientation of the magnetic field. © 2014 AIP Publishing LLC. [<http://dx.doi.org/10.1063/1.4903060>]

In the field of ferromagnetism, magnetic thin films with perpendicular magnetic anisotropy (PMA) are an important research subject. This is primarily related to their relevance in information technology since the advent of perpendicular magnetic recording,^{1–4} even if PMA films have been a crucial test case for fundamental research as well due to the opposing effects of magneto-crystalline anisotropy and magnetostatic self-interaction, which causes the occurrence on non-uniform microscopic magnetization states.^{5–19} The large amount of work on PMA films has led to an apparently very complete understanding of their micromagnetic states and magnetization reversal. Hereby, it is remarkable that the overwhelmingly vast majority of these studies either utilize in-plane or out-of-plane orientation of the magnetic field only, but not any intermediate field angles,^{20–28} even if the magnetization reversal processes for in-plane and out-of-plane applied fields are qualitatively very different. Furthermore, these intermediate field angles are of crucial relevance in magnetic recording as the key technological application of PMA films.^{29,30} Therefore, we have studied the angle-dependent magnetization reversal for epitaxial Co (0001) samples with PMA in the present work.

Epitaxial Co samples were grown by means of DC sputtering in an ultra high vacuum sputter system onto hydrofluoric acid etched Si(111) substrates. As shown in the inset of Fig. 1, we first deposited 12 nm Ag(111) and subsequently 50 nm Ti(0001) onto the silicon substrate as a template for the growth of epitaxial hcp Co with out-of-plane c-axis orientation, which is the magneto-crystalline easy axis,³¹ after which each sample was coated with 10 nm of amorphous SiO₂ to prevent surface oxidation. In our experiments, the Co film

thickness t_{Co} was varied between 100 nm and 400 nm. The crystallographic analysis of our epitaxial Co samples was carried out using x-ray diffraction. Macroscopic magnetization measurements were performed using a MicroMag vibrating sample magnetometer, which is equipped with a 360° rotational stage with a precision of better than 1°. Remanent magnetic domain pattern of our samples were measured via tapping mode magnetic force microscopy (MFM). Figure 1 shows a representative θ - 2θ x-ray diffraction pattern for one of our Co(0001) samples with $t_{\text{Co}}=200$ nm. The Co(0002) peak is clearly visible and together with the presence of the Ag(111) and Ti(0002) peaks, as well as the absence of any other peak, indicates the crystallographic quality and orientation of the deposited layers. For the 200 nm thick Co(0001) film, we estimated the average crystallite size to approximately 25.8 ± 0.5 nm by applying the Scherrer equation to the width of the Co(0002) diffraction peak.

Figure 2 shows a comparison of the in-plane and the out-of-plane magnetization curves $M(H)$ for a $t_{\text{Co}}=200$ nm sample. The experimental data are normalized to the

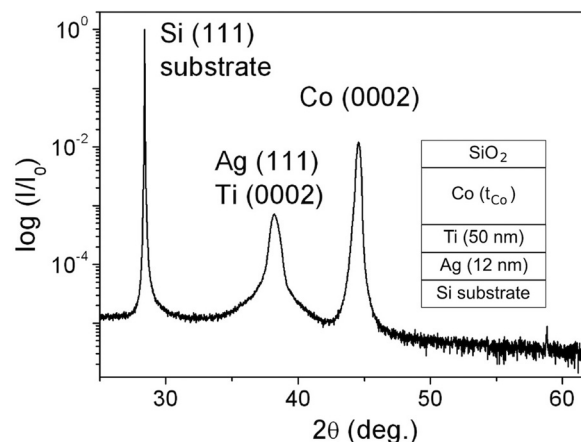


FIG. 1. X-ray diffraction pattern for a 200 nm thick Co film; the inset shows a schematic of the growth sequence used here.

^{a)}Present addresses: Laboratory for Mesoscopic Systems, Department of Materials, ETH Zurich, 8093 Zurich, Switzerland and Laboratory for Micro- and Nanotechnology, Paul Scherrer Institute, 5232 Villigen PSI, Switzerland.

^{b)}Present address: Institute for Complex Systems Simulation, University of Southampton, Southampton, SO17 1BJ, United Kingdom.

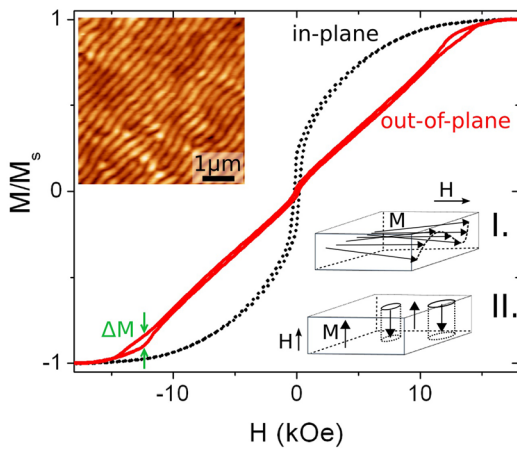


FIG. 2. In-plane (black dotted line) and out-of-plane (red solid line) hysteresis loops measured for a 200 nm thick epitaxial Co(0001) film; the left-hand inset displays an MFM image measured after in-plane demagnetization in an oscillating magnetic field of gradually reduced amplitude; the upper right-hand inset I shows a schematic of the soft spin wave mode; the lower right-hand inset II displays a schematic of the domain nucleation process. The meaning of the quantity ΔM is indicated by the solid green arrows.

saturation magnetization M_s and the diamagnetic substrate signal has been subtracted. Both curves exhibit a rather small hysteresis effect and only small remanent magnetization, which is typical for PMA films due to the occurrence of magnetic stripe domains,⁵ which we also find in our samples as demonstrated by the MFM-picture inset of Fig. 2. However, there are also very significant differences in between the in-plane and the out-of-plane magnetization curves. While the out-of-plane curve is nearly linear in its appearance, the in-plane data have a curved shape. Furthermore, the out-of-plane curve exhibits hysteresis only near saturation, while no visible hysteresis is apparent in the center, which gives the out-of-plane curve a quite anomalous shape. In contrast, the in-plane data exhibit a central hysteretic part around the origin. Both these curve shapes are documented in the literature and well understood.⁵

As one lowers the applied magnetic field for the in-plane orientation starting at high field values, one also lowers the energy of spin waves that describe an up-down oscillation of the magnetization, as shown in the inset I of Fig. 2. Due to PMA, the energy of these spin waves is reduced and they can actually reach zero energy,¹⁴ even in a finite applied field H_{cr} , which means that the uniform magnetization state becomes unstable at this critical field strength.³² Correspondingly, the film occupies a state with alternating tilted magnetization for $H < H_{cr}$ as its ground state, which actually resembles the soft spin wave state (inset I in Figure 2) and is a precursor to stripe domain structures at remanence. As the applied field is further reduced, the out-of-plane magnetization modulation of this state increases, while correspondingly the in-plane magnetization reduces, which leads to the overall curved appearance of the in-plane M vs. H behavior in Fig. 2. This magnetic state evolution also results in a finite remanent magnetization because even in remanence, the micromagnetic structure has an overall in-plane component, which has been aligned by the applied field sequence.²⁰ This alignment then results in a small central hysteresis of the

in-plane $M(H)$ curve, because these in-plane magnetization components require a small reverse field to be inverted.

For the out-of-plane magnetic field orientation measurement in Fig. 2, the before mentioned spin wave instability does not occur. Instead, the magnetization curve has basically three segments. The high field segments for $|H| > H_s \approx 13$ kOe are simply uniformly out-of-plane magnetized states. The intermediate state for $-H_s < H < H_s$ is nearly linear with up and down domains occurring in a field dependent proportion to minimize the total magnetostatic energy. Correspondingly, no hysteresis is present in the central portion of the magnetization curve.³³ However, minority domains cannot simply appear or disappear at the saturation field H_s , because their creation requires an activation energy, so that two separated hysteretic segments (ΔM) near $H = \pm H_s$ occur. A schematic of this reversal domain nucleation process is shown in the inset II of Fig. 2.

Overall, this now means that the magnetization processes that occur for the in-plane and out-of-plane magnetic field orientations describe fundamentally different transitions from the saturated state to the domain state. While the in-plane process proceeds via the instability of the uniform magnetization state, and thus is a second order phase transition, the out-of-plane process requires activated nucleation and thus represents a first order phase transition. Correspondingly, it is not at all trivial to predict what will happen for intermediate magnetic field angles.

In order to investigate this intermediate regime, we have measured $M(H)$ curves for different applied field angles β in between $\beta = 0^\circ$ and $\beta = 120^\circ$ in steps of 5° , with $\beta = 0^\circ$ corresponding to in-plane field orientation. Given that the specific appearance of hysteresis is a very good indicator for the above discussed two reversal mechanisms, we have extracted from our data the normalized difference in magnetization: $\Delta M/M_s = (M(H_{desc}) - M(H_{asc}))/M_s$, where $M(H_{desc})$ and $M(H_{asc})$ refer to the descending and ascending branches of our hysteresis loops. The meaning of ΔM is also graphically displayed in Fig. 2. Figure 3(a) shows a color-coded map of $\Delta M/M_s(\beta, H)$ for the sample with $t_{Co} = 200$ nm. Two types of hysteretic behavior appear as increased amplitudes of $\Delta M/M_s$ in this plot. The low magnetic field hysteresis defines a central band of enhanced $\Delta M/M_s(\beta, H)$ -values that is clearly visible in the proximity of $\beta \approx 0^\circ$ and virtually absent for $\beta \approx 90^\circ$. The domain nucleation hysteresis, on the other hand, is represented by the two high field $\Delta M/M_s(\beta, H)$ islands in proximity to H_s . These islands are most pronounced near $\beta = 90^\circ$. They reduce gradually by shifting β away from the out-of-plane orientation and they completely disappear for $\beta < 60^\circ$. This is a key observation of our work: The low field domain inversion hysteresis is practically always present, while the nucleation associated hysteresis is limited to $\beta > 60^\circ$ in our 200 nm thick Co film. Figure 3(b) shows the same type of data for a 400 nm thick Co(0001) film. We find that essentially the same type of behavior occurs, even if details are slightly modified due to the fact that the increased film thickness allows for a better minimization of the magneto-static self-energy, which stabilizes and extends the domain state regime.

In order to further investigate this characteristic change in the hysteretic behavior that occurs at a critical angle β in

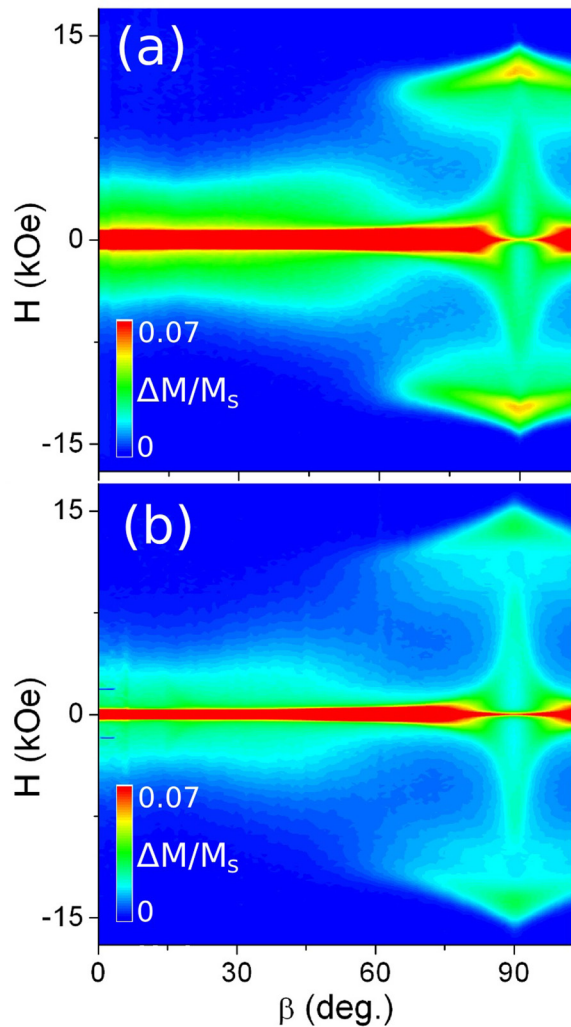


FIG. 3. $\Delta M/M_s(\beta, H)$ plots for Co(0001) film samples with 200 nm (a) and 400 nm (b) thickness, visualizing the hysteretic regions of the magnetic reversal process; the corresponding color codes are defined in each figure. Here, $\beta = 0^\circ$ and $\beta = 90^\circ$ correspond to in-plane and out-of-plane orientation of the magnetic field, respectively.

these Co(0001) films, we have analyzed the magnetic data in more detail. Figure 4(a) shows a color-coded plot of the magnetic susceptibility dM/dH , calculated from our M vs. H data via numerical differentiation as a function of applied field strength H and angle β , in conjunction with the hysteretic pattern from Fig. 3(a), which are shown as black contour lines. The occurrence of a non-vanishing susceptibility now indicates that the PMA Co-film is not saturated anymore, but instead has formed a non-uniform state. Correspondingly, the line at which the susceptibility changes from zero to non-vanishing values is a phase line where the system undergoes a phase transition. This happens at an approximately constant field value of about 8–9 kOe for the field orientation range $0^\circ < \beta < 60^\circ$, where the contrast in Fig. 4(a) changes from white to dark. It is important to notice that in this H - β regime no hysteresis is visible, which means that the magnetic system undergoes a second order phase transition here, driven by the instability of the uniform state. For magnetic field angles $\beta > 60^\circ$, the behavior is very different. Here, we observe the susceptibility and the hysteresis to occur nearly simultaneously, which is the hallmark of a first order

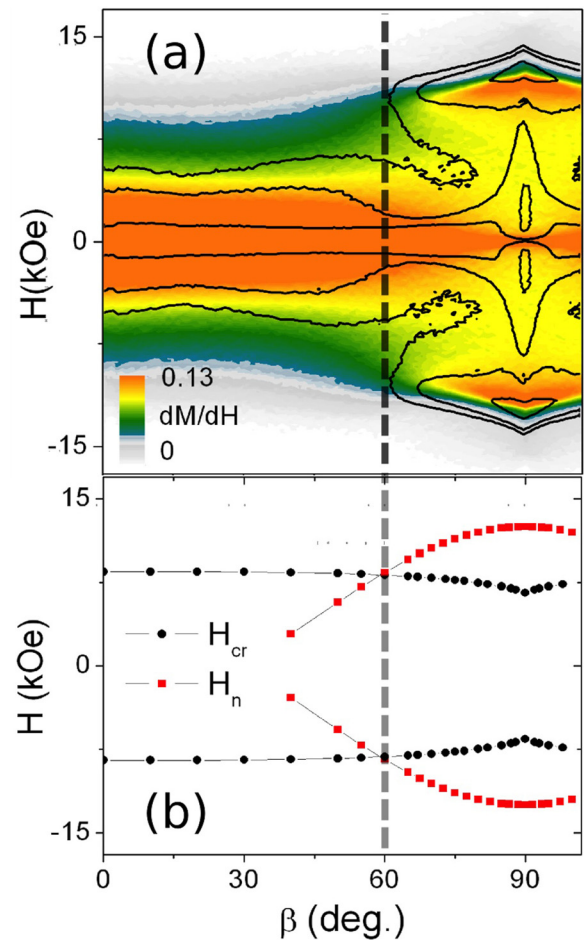


FIG. 4. (a) Magnetic susceptibility dM/dH determined from the nucleation branches of hysteresis loops for a $t_{\text{Co}} = 200$ nm sample as a function of the angle (β) and strength (H) of the applied magnetic field (values of dM/dH are normalized to (M_s/H_s)); for comparison the plot also displays the contours of $\Delta M/M_s(\beta, H)$ as black lines; (b) calculated $H_{\text{cr}}(\beta)$ and $H_{\text{n}}(\beta)$ curves for a 200 nm thick film with a uniaxial magneto-crystalline anisotropy field of $H_{\text{u}} = 11$ kOe; the angle β_{c} associated with the qualitative change in magnetization reversal behavior is indicated by a dashed line.

phase transition, in which the uniform magnetization state remains metastable, but is being depopulated. The slight shift that can be observed in between the hysteresis and the susceptibility features simply comes from the fact that occurrence of hysteresis indicates a delayed phase transition. This causes the visible effect that the susceptibility features are shifted to smaller field values, because the plot data are extracted from the nucleation branches of the hysteresis loops.

To corroborate this interpretation, we have calculated the orientation dependence for the critical field H_{cr} , at which the spin wave instability occurs, and for the nucleation field H_{n} , at which reverse domain nucleation starts. The results of these calculations, which are based on well-established models,⁵ are shown in Fig. 4(b).³⁴ For the in-plane magnetic field configuration, we find $H_{\text{cr}} \approx 8.5$ kOe and upon increasing β , H_{cr} remains nearly constant up to about 50° and subsequently decreases slightly to approximately 6.5 kOe for $\beta = 90^\circ$. Thus, the spin wave instability does not show a very substantial angular dependence.³⁵ The nucleation field H_{n} , on the other hand, shows a distinctively different behavior. It exhibits a clear maximum of $H_{\text{n}} \approx 12.5$ kOe at $\beta = 90^\circ$ and falls off substantially upon reducing β . Actually, no positive

value H_n exists for small β , which is easy to understand. The nucleation of a reverse domain in a positive field is driven by a reduction of the magnetostatic self-energy, because only this energy term can be lowered via nucleation against the applied field direction. For an in-plane oriented uniform state, however, the magnetostatic energy vanishes and thus, cannot be further reduced. Correspondingly, nucleation cannot occur for positive applied field values.

So, according to our model calculations, it is the reverse domain nucleation process that triggers the qualitative change of behavior here, because it is a highly effective process for (nearly) out-of-plane field orientations, while it is completely ineffective near in-plane orientations of the magnetic field. This produces the crossing of the $H_{cr}(\beta)$ and $H_n(\beta)$ curves near $\beta = 60^\circ$, which changes the magnetization reversal in a fundamental manner. Whenever $H_{cr} > H_n$, the magnetization reversal is initiated via the spin wave instability, and nucleation never occurs, while for $H_{cr} < H_n$ magnetization reversal is initiated by the nucleation process before any instability can occur. This distinct angular dependence of H_n and H_{cr} , in conjunction with the fact that the $H_{cr}(\beta)$ -line describes a second order phase boundary, while the $H_n(\beta)$ -curve is associated with a first order phase transition also indicates that the transition point at $\beta = 60^\circ$ actually identifies a *tricritical point*. Crucially, the magnetization reversal changes at this point in a qualitatively manner, going from a thermally assisted nucleation process near normal field orientation to an instability driven decay near in-plane field orientation. Accordingly, the dynamic evolution of the reversal process will also be modified via the field angle, which is of course a crucial aspect of high-speed magnetic information storage such as magnetic recording.

In summary, we have studied magnetization reversal in epitaxial Co (0001) thin films with perpendicular magnetic anisotropy as a function of the applied field angle β . Hereby, we observe two very different magnetization reversal regimes. For $\beta < 60^\circ$, we find the onset of the domain phase to be hysteresis free, while for $\beta > 60^\circ$, the occurrence of the domain phase is accompanied by hysteresis. The underlying mechanisms for these different behaviors are analyzed and corroborated by means of model calculations, leading to the conclusion that the phase diagram of PMA films, such as the investigated Co (0001) films, is more complex than previously anticipated, and furthermore implies most relevant consequences for the dynamic behavior of magnetization reversal in PMA films.

We acknowledge funding from the Basque Government (Program No. PI2012-47) and the Spanish Government (Project No. MAT2012-36844). O.I. acknowledges the Basque Government for support from Grant No. BFI09.284. Work at UTFSM was supported by FONDECYT 1120618 and from ICM P10-06-F funded by Fondo de Innovación para la Competitividad, from the MINECON.

¹R. Wood, *IEEE Trans. Magn.* **36**, 36 (2000).

²J. P. Wang, W. K. Shen, J. M. Bai, R. H. Victora, J. H. Judy, and W. L. Song, *Appl. Phys. Lett.* **86**, 142504 (2005).

³D. Suess, T. Schrefl, S. Faehler, M. Kirschner, G. Hrkac, F. Dorfbauer, and J. Fiedler, *Appl. Phys. Lett.* **87**, 012504 (2005).

- ⁴A. Berger, N. Supper, Y. Ikeda, B. Lengsfeld, A. Moser, and E. E. Fullerton, *Appl. Phys. Lett.* **93**, 122502 (2008).
- ⁵A. Hubert and R. Schäfer, *Magnetic Domains* (Springer, 2000).
- ⁶C. Kittel, *Rev. Mod. Phys.* **21**, 541 (1949).
- ⁷M. W. Muller, *Phys. Rev.* **122**, 1485 (1961); W. F. Brown, Jr., *Phys. Rev.* **124**, 1348 (1961).
- ⁸P. F. Carcia, A. D. Meinhaldt, and A. Suna, *Appl. Phys. Lett.* **47**, 178 (1985).
- ⁹C. Chappert, K. Le Dang, P. Beauvillain, H. Hurdequint, and D. Renard, *Phys. Rev. B* **34**, 3192 (1986).
- ¹⁰C. Liu, E. R. Moog, and S. D. Bader, *Phys. Rev. Lett.* **60**, 2422 (1988).
- ¹¹Y. Yafet and E. M. Gyorgy, *Phys. Rev. B* **38**, 9145 (1988).
- ¹²J. R. Dutcher, B. Heinrich, J. F. Cochran, D. A. Steigerwald, and W. F. Egelhoff, Jr., *J. Appl. Phys.* **63**, 3464 (1988).
- ¹³R. Allenspach, M. Stampanoni, and A. Bischof, *Phys. Rev. Lett.* **65**, 3344 (1990).
- ¹⁴R. L. Stamps and B. Hillebrands, *Phys. Rev. B* **43**, 3532 (1991).
- ¹⁵Z. Q. Qiu, J. Pearson, and S. D. Bader, *Phys. Rev. Lett.* **70**, 1006 (1993).
- ¹⁶A. Berger and H. Hopster, *Phys. Rev. Lett.* **76**, 519 (1996).
- ¹⁷E. Y. Vedmedenko, H. P. Oepen, A. Ghazali, J.-C. S. Lévy, and J. Kirschner, *Phys. Rev. Lett.* **84**, 5884 (2000).
- ¹⁸O. Portmann, A. Vaterlaus, and D. Pescia, *Nature* **422**, 701 (2003).
- ¹⁹N. Saratz, A. Lichtenberger, O. Portmann, U. Ramsperger, A. Vindigni, and D. Pescia, *Phys. Rev. Lett.* **104**, 077203 (2010).
- ²⁰M. Hehn, S. Padovani, K. Ounadjela, and J. P. Bucher, *Phys. Rev. B* **54**, 3428 (1996).
- ²¹M. Hehn, K. Ounadjela, J.-P. Bucher, F. Rosseaux, D. Decanini, B. Bartenlian, and C. Chappert, *Science* **272**, 1782 (1996).
- ²²S. Hameed, P. Talagala, R. Naik, L. E. Wenger, V. M. Naik, and R. Proksch, *Phys. Rev. B* **64**, 184406 (2001).
- ²³M. Kisielewski, A. Maziewski, M. Tekielak, J. Ferré, S. Lemerle, V. Mathet, and C. Chappert, *J. Magn. Magn. Mater.* **260**, 231 (2003).
- ²⁴O. Donzelli, M. Bassani, F. Spizzo, and D. Palmeri, *J. Magn. Magn. Mater.* **320**, e261 (2008).
- ²⁵J. Brandenburg, R. Hühne, L. Schultz, and V. Neu, *Phys. Rev. B* **79**, 054429 (2009).
- ²⁶S. R. Bakaul, W. Lin, and T. Wu, *Appl. Phys. Lett.* **99**, 042503 (2011).
- ²⁷J. Gao, S. Tang, Y. Li, W. Xia, T. Tang, and Y. Du, *J. Appl. Phys.* **112**, 073913 (2012).
- ²⁸N. Berggaard, J. P. Jamet, A. Mougin, J. Ferré, J. Gierak, E. Bourhis, and R. Stamps, *Phys. Rev. B* **86**, 094431 (2012).
- ²⁹K. Z. Gao, O. Heinonen, and Y. Chen, *J. Magn. Magn. Mater.* **321**, 495 (2009).
- ³⁰H. Katada, M. Hashimoto, Y. Urakami, S. Das, M. Shiimoto, M. Sugiyama, T. Ichihara, H. Hoshiya, K. Tanahashi, and K. Nakamoto, *IEEE Trans. Magn.* **46**, 798 (2010).
- ³¹H. Gong, M. Rao, D. E. Laughlin, and D. N. Lambeth, *J. Appl. Phys.* **85**, 4699 (1999).
- ³²It can be shown that the spin waves relevant to the instability process are those for which the angle between the in-plane magnetization and the wave vector is equal to $\pi/2$. In this case, the dispersion relation is given by $\omega(\vec{k}) = \gamma[W_x(\vec{k})W_y(\vec{k})]^{1/2}$, with $W_x(\vec{k}) = H \cos(\beta - \phi) - M_{eff} \sin^2 \phi + 4\pi M_s g(k) + D_x k^2$, $W_y(\vec{k}) = H \cos(\beta - \phi) + M_{eff} \cos(2\phi) - 4\pi M_s g(k) \cos^2 \phi + D_x k^2$, and $g(q) = 1 - (1 - e^{-q})/q$. Hereby, k is the (in-plane) wave vector of the spin waves, M_s is the saturation magnetization, $M_{eff} = 4\pi M_s - H_u$ is the effective magnetization, with $H_u > 0$ being the amplitude of the perpendicular uniaxial anisotropy field ($H_u = 2K_u/M_s$). Furthermore, $D_x = 2A/M_s$ is the exchange stiffness, γ is the gyromagnetic ratio, and t is the film thickness. The angle between the film plane and the equilibrium magnetization is ϕ , and β denotes the angle between the film plane and the DC applied field. For further details, see P. Landeros, R. E. Arias, and D. L. Mills, *Phys. Rev. B* **77**, 214405 (2008).
- ³³The small hysteresis effect and enhanced susceptibility near zero magnetic field is the commonly observed result of imperfect domain expansion and contraction, which is related to the existence of sample defects. See, for instance, A. Berger, A. W. Pang, and H. Hopster, *Phys. Rev. B* **52**, 1078 (1995).
- ³⁴For our calculations, we assume the saturation magnetization of Co to be $M_s = 1440 \text{ emu/cm}^3$ and our films to exhibit a perpendicular magnetic anisotropy field of $H_u = 2K_u/M_s = 11 \text{ kOe}$. We then determine for every magnetic field orientation β the quantity H_{cr} as the highest field strength, at which a zero energy spin-wave excitation is observed for the uniform magnetization state. For the calculation of the nucleation field H_n , we determined for every magnetic field orientation β the activation barrier E_n as a function of the applied field strength H for a circular nucleus of inverted magnetization, i.e., being magnetized along $\beta + 180^\circ$ inside the nucleus,

while the background magnetization remains oriented along β . We then estimate the activation energy accessible under our experimental condition by matching the E_n vs. H curve for normal field orientation, i.e., $\beta = 90^\circ$, to the experimentally observed nucleation field. Using this fixed $E_{n(\text{ref.})}$ value, we then determine H_n for all other β as the intercept of the respective E_n vs. H curves with $E_{n(\text{ref.})}$.

³⁵The specific nature of the spin wave instability changes as a function of β , because the nature of the destabilizing energy changes. While the PMA triggers the instability for the in-plane orientation, because it is the energy that is not minimized in this case, the magnetostatic energy is responsible for the spin wave softening in the out-of-plane direction, because it is the energy term that can get lowered by doing so in this case.